Published in final edited form as:
Neuron. 2012 December 20; 76(6): 1189–1200. doi:10.1016/j.neuron.2012.10.036.

Hilar Mossy Cell Degeneration Causes Transient Dentate Granule Cell Hyperexcitability and Impaired Pattern Separation

Seiichiro Jinde[1,3,6], **Veronika Zsiros**[1,6], **Zhihong Jiang**[1], **Kazuhito Nakao**[1], **James Pickel**[2], **Kenji Kohno**[4], **Juan E. Belforte**[1,5], and **Kazu Nakazawa**[1,*]

[1]Unit on Genetics of Cognition and Behavior, National Institute of Mental Health, National Institutes of Health, Department of Health and Human Services, Bethesda, MD 20892, USA

[2]Transgenic Core Facility, National Institute of Mental Health, National Institutes of Health, Department of Health and Human Services, Bethesda, MD 20892, USA

[3]Department of Neuropsychiatry, Graduate School of Medicine, University of Tokyo, Tokyo 113-8655, Japan

[4]Laboratory of Molecular and Cell Genetics, Graduate School of Biological Sciences, Nara Institute of Science and Technology, Nara 630-0192, Japan

Summary

Although excitatory mossy cells of the hippocampal hilar region are known to project both to dentate granule cells and to interneurons, it is as yet unclear whether mossy cell activity's net effect on granule cells is excitatory or inhibitory. To explore their influence on dentate excitability and hippocampal function, we generated a conditional transgenic mouse line, using the Cre/*loxP* system, in which diphtheria toxin receptor was selectively expressed in mossy cells. One week after injecting toxin into this line, mossy cells throughout the longitudinal axis were degenerated extensively, theta wave power of dentate local field potentials increased during exploration, and deficits occurred in contextual discrimination. By contrast, we detected no epileptiform activity, spontaneous behavioral seizures, or mossy-fiber sprouting 5–6 weeks after mossy cell degeneration. These results indicate that the net effect of mossy cell excitation is to inhibit granule cell activity and enable dentate pattern separation.

Keywords

Cre recombinase; dentate excitability; diphtheria toxin; genetic cell ablation; inducible transgenic mice; mossy fiber sprouting; pattern separation; temporal lobe epilepsy

Introduction

Located in the hilar region of the mammalian hippocampal dentate gyrus, glutamatergic mossy cells receive convergent synaptic input from dentate granule cells, semilunar granule

*Correspondence: nakazawk@mail.nih.gov.
[6]These authors contributed equally to this work
[5]Present address: Systems Neuroscience Group, Department of Physiology, School of Medicine, University of Buenos Aires, Argentina

The authors declare no conflict of interest.

cells, local inhibitory interneurons, and septal neurons (Amaral 1978; Frotscher et al. 1991; Soriano and Frotscher 1994; Lübke et al. 1997; Williams et al. 2007). Their associational and commissural axonal projections, in fact, innervate proximal dendrites of granule cells and inhibitory interneurons all along the longitudinal axis of the inner molecular layer (IML) of the dentate gyrus (Seress and Ribak 1984; Amaral and Witter 1989; Deller et al. 1994; Wenzel et al. 1997; Zappone and Sloviter 2001). While early *in vivo* electrophysiological studies consistently found that excitatory commissural fibers from mossy cells activate inhibitory neurons and inhibit granule cells (Buzsáki and Eidelberg 1981, 1982; Douglas et al. 1983; Bilkey and Goddard 1987), however, it has recently been suggested that under normal conditions, their net effect is excitatory (Ratzliff et al. 2004; Myers and Scharfman 2009). The excitatory hypothesis is consistent with electron microscopy data indicating that >90% of the total synapses formed by a mossy cell in the IML are on dendritic spines of granule cells (Buckmaster et al. 1996; Wenzel et al. 1997), and there has also been considerable debate about mossy cells' role in the limbic genesis of epilepsy.

Loss of hilar neurons including mossy cells and inhibitory interneurons is, in fact, characteristic in such pathologies as epilepsy (Margerison and Corsellis 1966; Sloviter 1987; Blümcke et al. 2000) and brain injury (Lowenstein et al. 1992; Santhakumar et al. 2001; Johansen et al. 1987; Hsu and Buzsáki 1993), and extensive loss of these cells following seizures or head trauma is associated with immediate granule cell hyperexcitability (Sloviter 1983; Lowenstein et al. 1992; Toth et al. 1997). Yet whether mossy cell loss is responsible for this observed granule cell hyperexcitability is not known.

According to the "dormant basket cell" hypothesis, because mossy cells normally excite inhibitory basket cells to inhibit granule cells, their loss should lead to granule cell hyperexcitability and spontaneous granule cell epileptiform behavior (Sloviter 1991; Sloviter et al. 2003). The "irritable mossy cell" hypothesis (Santhakumar et al. 2000; Ratzliff et al. 2002), by contrast, holds that following injury, surviving mossy cells hyperexcite granule cells by sending uncontrolled excitatory feedback. Because it was not possible to eliminate mossy cells selectively until now, researchers were unable to test these hypotheses *in vivo*.

To determine how selective and extensive loss of mossy cells affects the excitability and behavior of dentate granule cells, we developed a toxin-mediated, mossy cell-specific ablation mouse line in which mossy cells selectively express the diphtheria toxin (DT) receptor. In these mutants, following DT treatment ~75% of mossy cells degenerate rapidly. To evaluate granule cell excitability after degeneration, we recorded local field potential (LFP) activity *in vivo* and assessed dentate gyrus hippocampal slices for synaptic reorganization believed to be triggered by mossy cell loss (Jiao and Nadler 2007). Context-discrimination tasks were used to assess pattern separation.

Results

Mouse line with restricted expression of diphtheria toxin receptor in hilar mossy cells

To generate hilar mossy cell-specific transgenic mice, we co-injected Cre recombinase cDNA with a minimal promoter element and a DNA fragment containing 5′-transcriptional regulatory region of calcitonin receptor-like receptor (*Crlr*) gene (see Figure S1A available online) into fertilized eggs from the C57BL/6N strain. After crossing with a *loxP*-flanked Rosa26*lacZ* reporter mouse, a transgenic line Cre #4688 (*mossy cell/CA3-Cre*) at 8 weeks old shows *lacZ*-positive somata exclusively in the dentate hilus and area CA3 pyramidal cells, with almost none in the dentate granule cell layer, area CA1, or neocortex (Figures 1A and S1A). Homogenous staining of the IML where mossy cell axons terminate (Blackstad 1956; Amaral and Witter 1989) reveals intense Cre-immunoreactivity (-IR) throughout the

dentate hilus but not in the CA3 pyramidal cell layer (Figure 1B). *LacZ*-positive cells appear in hilus/CA3c by postnatal day 9 and remain stable to at least 25 weeks, while ~20% cells in the CA3b pyramidal cell layer are Cre-positive (Figure S1A). *LacZ* co-expression in over 90% of hilar cells positive for the murine mossy cell markers calretinin (CR) or GluA2/3 (Liu et al. 1996; Leranth et al. 1996) further confirms Cre recombination in hilar mossy cells, while *LacZ*-IR never occurs with GAD67-IR (Figure 1C).

We also generated *loxP*-flanked diphtheria toxin receptor (fDTR) transgenic mouse lines under the control of a CaMKIIα promoter, in which the human homologue of heparin-binding epidermal growth factor-like growth factor (HB-EGF) functions as a DTR in mice (Saito et al., 2001). HB-EGF (DTR) is expressed upon excision of an alkaline phosphatase-pA cassette by Cre/*loxP* recombination (Figure S1B). In the fDTR *line B* at 8 weeks of age, alkaline phosphatase staining is robust in the entire forebrain and partial midbrain, but absent in brainstem and cerebellum (Figure 1D). Notably, from 8 weeks (Figure 1D) to 20 weeks (Figure S1C), staining in hippocampal area CA3 is minimal compared to that in the dentate gyrus, mossy fibers, and area CA1, suggesting negligible expression of the transgene in CA3 pyramidal neurons after Cre recombination. To confine DTR expression to hilar mossy cells specifically, we crossed the fDTR-B line with the afore-mentioned mossy cell/CA3-Cre line to generate the mossy cell-DTR line, $Cre^{+/-}$; $DTR^{loxP/-}$ (hereafter referred to as *mutant*).

Mossy cell degeneration after treatment with diphtheria toxin

To determine whether DTR causes mossy cells to degenerate *in vivo,* we injected DT *i.p.* on two consecutive days in mutant males (8–20 week-old) and their age-matched controls of the Cre, fDTR, or C57BL/6 (B6) wild-type genotypes. Three measures were used to assess the specificity and magnitude of DT-induced effects on mossy cells: cell shape, assessed by Nissl (Safranin O) staining; degree of degeneration, assessed by Fluoro-Jade B (FJB) staining (Schmued and Hopkins, 2000); and positive cell numbers for mossy cell markers, GluA2/3 and CR, in the hilus. One week after DT injection, the presence of hilar cells with pyknotic nuclei and less-stained cytoplasm in Nissl-stained sections (Figure 2) shows that mossy cell neurodegeneration is already robust. Four to 6 weeks after DT, neurodegeneration leads to a net loss of hilar cells in both dorsal and ventral blades (data not shown). Cells that remain 4–6 weeks post-DT carry small nuclei and appear to be interneurons or glial cells.

FJB staining confirms this neurodegeneration. In the mutants 5 to 7 days after initial DT injection, prominent FJB-positive staining is evident in both area CA3 and the hilus but not in the granule cell layer (Figure 3A, middle panel). DT-treated control mice, regardless of genotype, show no FJB staining (Figure 3A, left panel). Four weeks later, the hilus and IML mossy-cell target zone are consistently FJB-positive, presumably reflecting degenerated mossy cell axons (Figure 3A, right panel). Notably, we detected no FJB staining of any axon plexus in the outer molecular layer or in the granule cell layer, and at this time point, few large somata in the hilar region are visibly stained.

Examining for staining of mossy cells and inhibitory interneuron markers at 1 and 4 weeks following DT treatment, we found no significant difference between saline-treated mutant and control mice in number of GluA2/3-, CR-, and neuropeptide Y (NPY)-positive cells throughout the hilar region. Since these IRs are not significantly altered by DT treatment in the dorsal or ventral hilus in controls (Figure S2B), and there is no difference among control genotypes in number of hilar GluA2/3-, CR-, and neuropeptide Y (NPY)-positive cells (Figure S2C), we combined data from our three control genotypes (Cre, fDTR, and B6 wild-type) to form our combined control (control) group.

In mutants one week after DT treatment, the number of GluA2/3-positive cells in the hilus of the dorsal hippocampus decreases to 26.1%, and by 4 weeks after treatment to 9.5% compared to numbers in DT-treated controls (Figures 3B to 3D). Similarly, the number of GluA2/3-positive cells in the ventral hilar region in mutants decreases to 27.9% of that in controls by week one and to 10.5% by week four following DT treatment. The number of CR-positive hilar cells in mutants decreases by week one to 79.9% and by week four to 6.7% compared to levels found in controls. By contrast, 4 weeks after DT treatment mutants show no obvious effect on the interneuron marker NPY-IR in the dorsal or ventral hilus (Figures 3C and 3D).

Different rates of reduction in GluA2/3- and CR-positive hilar cells following DT treatment may arise from variability in protein degradation. While GluA2/3- and CR-positive mossy cells mostly overlap (Figure S2A; see Fujise et al. 1998), one week after DT treatment the number of GluA2/3- and CR-positive ventral hilar cells originating from the same mutant brain tissues varies widely (Figure 3B). In contrast, DT treatment does not obviously affect the interneuron marker NPY-IR in the dorsal or ventral hilus in mutants (Figures 3C and 3D).

Since hilar neurodegeneration is already prominent one week after DT treatment (Figure 2 and Figure 3A), loss of GluA2/3 mossy-cell-marker labeling is likely to be a signature of mossy cell neurodegeneration. If so, our results show that in mutants, ~75% of mossy cells are selectively degenerated 7 days after DT treatment and ~90% by 4 weeks post-DT. To assess the acute effects of functional mossy cell loss, we performed experiments at 4–11 days (*acute phase*); and to assess the chronic effects, at 4–6 weeks (*chronic phase*) after DT treatment.

Cre-recombination also occurs in CA3c pyramidal neurons (Figures 1A and S1A), whose axons may project, either directly or via mossy cells, to dentate granule cells (Scharfman 2007; Wittner et al. 2007). To test whether residual DTR expression ablates CA3c pyramidal neurons in DT-treated mutants, we compared the number of NeuN-positive pyramidal neurons before DT treatment and one week after (Figure 3E) and found no significant difference between DT-treated mutants and controls—unlike NeuN-positive cells in the hilar region, which are significantly more reduced in number 7 days after DT treatment in mutants than in controls. These findings show that DT treatment affects the integrity of area CA3c only minimally and confirm that in our mutant line, DT-mediated cell ablation is mossy-cell selective.

Mossy cell degeneration reduces both excitatory and inhibitory inputs to granule cells

Finding no significant difference among our control genotypes in spontaneous EPSC (sEPSC) and sIPSC events in dentate granule cells of DT-treated mutants (n=10) and controls (n=13) during the acute phase (post-DT 4–11 days) (Figure S2D), we again combined them into a single control group. DT treatment does not appear to affect sEPSC event amplitude (Figure 4B), rise times (20–80%; 1.57±0.15 ms for control, 1.71±0.18 ms for mutant, *t*-test, $p=0.62$) and decay times (66–30%; 6.79±0.43 ms for control, and 6.88±0.54 ms for mutant, *t*-test, $p=0.43$). For sIPSC events, too, amplitude (Figure 4B) and decay times (66–30%; 11.86±0.59 ms for control, and 11.97±0.40 ms for mutant, *t*-test, $p=0.93$) remained unchanged.

By contrast, following DT treatment the mean frequency of both sEPSC (Figure 4A) and sIPSC (Figure 3A) events is dramatically more reduced in mutants than in controls, even though the event properties in DT-untreated mutants (n=4, sEPSC frequency, 1.84±0.18 Hz; sEPSC amplitude, 6.78±0.54 pA; sIPSC frequency, 4.11±1.38 Hz; sIPSC amplitude, 15.48±1.67 pA) were similar to those in DT-treated controls. Consistent with earlier findings

(Scharfman 1995), these results confirm that mossy cells send both excitatory and inhibitory input directly to dentate granule cells and send disynaptic inhibitory input indirectly through local interneurons.

Mossy cells drive interneuronal inhibition of granule cells

To assess the extent to which mossy cells mediate synaptic inhibition in granule cells, we blocked glutamatergic transmission (with 10 μM APV and 20 μM NBQX) in slices in the acute phase following DT treatment (Figures 4C and 4D). In all genotypes, although sIPSCs were still recordable, the blockers abolished granule cell sEPSCs completely (Figure 4C). Blocking excitatory synaptic transmission in controls (n=10) does decrease sIPSC frequency to 72.7±7.5 % of the value before blocker application, or roughly the same level as in mutant mice (Figure 4C), while in DT-treated mutants, sIPSC frequency is unaffected (n=6, 100.3±3.3%; repeated measure of ANOVA, $F(2,13) = 4.12$, $p < 0.05$ for genotype effect).

These findings suggest that ipsilateral mossy cells mediate ≥30% of synaptic inhibition of granule cells. That spontaneous high firing of mossy cells constantly drives interneurons (Scharfman and Schwartzkroin 1988; Buckmaster et al. 1992; Zsiros et al. unpublished data) may account for the apparently negligible effect of excitatory inputs to other interneurons directly innervated by perforant path or mossy fibers. In all groups, these blockers leave sIPSC event amplitude (Figure 4D) and decay times (control, 11.5±1.5 ms before and 10.8±0.82 ms after the drug, paired *t*-test, $p=0.68$; mutant: 8.75±0.51 ms before and 8.97 ± 0.99 ms after the drug, $p=0.52$) unaffected, although sIPSCs are blocked completely by 12.5 μM gabazin (n=5, data not shown).

Analysis of granule cell 'rise times' for sIPSCs (20–80% rise times) (Figures 4A and 4B) reveals much faster rise times in DT-treated mutants (0.88±0.024 ms) than in DT-treated controls (1.37±0.064 ms) (*t*-test, $p < 0.02$). In a different animal cohort of brain slices, APV and NBQX application accelerated rise times in controls (n=10, 1.40±0.08 ms before vs 0.89±0.12 ms after drug) to levels found in DT-treated mutants, but when glutamatergic blockers were applied, rise times in DT-treated mutants did not change (n=6, 0.88±0.25 ms before vs 0.88±0.24 ms after drug; repeated measure of ANOVA, $F(2,13) = 6.22$, $p < 0.02$ for genotype effect). These findings suggest that at least 30% of the synaptic inhibition of granule cells is mediated by interneurons driven by mossy cells in our horizontal slice preparation. They further suggest that mossy cells may selectively target certain types of interneurons to slow this synaptic inhibition.

Examining long-term effects of mossy cell loss at the cellular level, we find that decreases in sEPSC and sIPSC event frequency disappear in the chronic phase in mutant granule cells (Figure 4E), suggesting functional compensation of excitatory and inhibitory inputs to granule cells. While delayed axonal sprouting of local interneurons (Figure 6C) may compensate for changes in sIPSC frequency, however, the compensation mechanism for changes in sEPSC frequency remains unclear. All genotypes show similar values for other parameters, such as sEPSC event amplitude (Figure 4F), rise time (20–80%; 1.43±0.16 ms for control, 1.17±0.10 ms for mutant, *t*-test, $p=0.05$) and decay time (66–30%; 8.30±0.41 ms for control, and 8.05±0.86 ms for mutant, *t*-test, $p=0.79$) or sIPSC amplitude (Figure 4F), rise time (20–80%; 1.46±0.40 ms for control, 1.10±0.22 ms for mutant, *t*-test, $p=0.42$), and decay time (66–30%; 11.40±0.72 ms for control, and 12.69±0.53 ms for mutant, *t*-test, $p=0.18$).

Mossy cell degeneration causes acute hyperexcitability in dentate granule cells

To determine granule cell responses to perforant pathway stimulation in acute (4-11 days post-DT) and chronic (6–8 weeks post-DT) phases of mossy cell degeneration, we first

measured field EPSP (fEPSP) amplitudes in hippocampal slices in response to low-intensity perforant path stimulation, which were then normalized by their fiber-volley amplitudes. In the acute phase, fEPSP amplitudes in mutants were much larger than those in DT-treated controls (Figure 5A). Interestingly, however, this increase appears to be transient, with mutant amplitudes returning to normal in the chronic phase.

Acute granule cell hyperexcitability is also reflected in the stimulation intensity thresholds for evoking population spikes (recorded extracellularly). While saline-treated mutants show no increase in dentate excitability (data not shown), population spike threshold is significantly lower in the acute (but not the chronic) phase of mossy cell degeneration (Figure 5B).

Assuming that an excitatory stimulus will cause more granule cells to discharge leading to more IEG expression in mutants than in controls, we next evaluated expression of the immediate-early gene (IEG) in response to kainic acid (KA) injection. As expected, in the acute phase KA injection (20 mg/kg *i.p.*) evokes expression of both Zif268 and c-Fos in more granule cells in mutants than in controls (Figures 5C to 5E), and regardless of genotype, no such expression occurs in the untreated condition. In the chronic phase, however, differences in IEG expression between mutants and controls is negligible [Zif268, 165.8±58.6 for control (n=8), 226.9±79.1 for mutant (n=7), *t*-test, p=0.54; c-Fos, 1766.5±557.7 for control, 2496.7±973.3 for mutant, *t*-test, $p=0.53$].

We also examined the intensity of KA-induced seizures in acute (Figure 5F) and chronic (Figure 5G) phases. With seizures scored every 5 min for one hour following *i.p.* injection of 20 mg/kg KA, the cumulative seizure score was significantly higher for mutant mice than for their control littermates during the acute phase (Figure 5F; 21.0±2.3 for control, 27.8±2.2 for mutant, *t*-test, $p<0.05$) but not during the chronic phase (Figure 5G; 18.2±3.0 for control, 19.4±2.5 for mutant, *t*-test, $p=0.75$). In mutants, the maximum seizure score was also significantly higher than in controls during the acute (2.4±0.2 for control, 3.2±0.3 for mutant, *t*-test, $p<0.05$) but not the chronic phase (1.8±0.3 for control, 2.3±0.3 for mutant, *t*-test, $p=0.38$). Taken together, these results demonstrate granule cell hyperexcitability in response to mossy cell degeneration during acute, but not chronic phase.

Absence of mossy-fiber sprouting and spontaneous seizure discharges

To see if granule cell axons sprout into denervated IML during chronic phase, as occurs when seizures induce hilar neuron loss (Jiao and Nadler 2007; Kienzler et al. 2009), we used Timm staining (Figure 6A) and zinc transporter 3 (ZnT3) immunostaining (Figure 6B) to visualize mossy fibers 6 weeks after DT treatment (n=6 mutants, n=5 controls). Surprisingly, following extensive mossy cell loss, mutant mice show no detectable mossy fiber sprouting in the IML of either dorsal or ventral hippocampus. Semi-quantitative analysis of Timm staining (Tauck and Nadler 1985) shows no statistical difference between genotypes (0.17±0.10 for controls, 0.13±0.08 for mutants, Mann-Whitney *U*-test, $p=0.80$). Despite mossy cell loss confirmed in mutants by diminished band-like staining in IML (whether by Timm or anti-ZnT3) identified as mossy cell axons in controls (West and Andersen 1980; Corbetta et al. 2009), moreover, Netrin G2-immunostaining (Nishimura-Akiyoshi et al. 2007) confirms the absence of detectable sprouting from perforant path axonal fibers (Figure S3A).

The fact that anti-choline acetyltransferase staining is similar in DT-treated mutants with excessive mossy cell loss and in DT-treated controls further suggests that mossy cell loss does not affect cholinergic projections to dentate gyrus (Figure S3B). Conversely, GAD67 immunostaining 4 weeks (but not 4–7 days) after DT treatment shows dense immunoreactivity in the IML (Figure 6C). Since we detect no mossy fiber sprouting in DT-

treated mutants' IML (Figures 6A and 6B), this sprouting appears to derive from GABAergic interneurons rather than from granule cells. Indeed, in the chronic phase, DT-treated mutants' reduced frequency of sIPSC events returns to levels found in controls (Figure 4C). Increased GABAergic sprouting to IML, which first appears 2 weeks after DT treatment, appears to reflect a slow compensatory process for increased excitability of granule cells.

To detect spontaneous events and seizure discharges, we recorded LFPs from the dentate gyrus in freely ambulant control and mutant mice in a circular open arena for 3 hr each day. Although the recording methods used can detect KA-induced epileptiform activity, mutants show no detectable epileptiform discharge up to 35 days after DT injection (Figure 6D), and multiple non-continuous observation periods (total 4-8 hr per day, n=9) revealed no spontaneous seizure-like behaviors. Selective mossy cell loss *in vivo,* therefore, does not appear to produce spontaneous epilepsy.

To analyze the impact of mossy cell loss on LFPs in the dentate gyrus, we placed electrodes at distances estimated from polarity reversal of "dentate spikes" during immobility (see Fig 7A; Bragin et al. 1995b) and histologically verified by electrolesions (Figure S4A). In comparison with the same animals/electrodes/behavioral state before and 4 weeks after DT treatment, LFP oscillatory powers at theta frequency (7–12 Hz) were enhanced during exploration in mutants one week from DT exposure (Figures 7B and 7C; MANOVA, $F(2,12)=4.10$ for day x genotype interaction, $p<0.05$). That no such changes occurred in DT-treated fDTR controls (Figure 7C) suggests that the transient increase in theta power in mutants is not due to DT treatment. DT injection shows no effect on LFP power spectra during immobility periods (Figure S4B) regardless of genotype. Since the theta input to the dentate gyrus *in vivo* is conveyed from entorhinal cortex by the perforant path to granule cells (Bragin et al. 1995a; Kocsis et al. 1999), transient elevation of theta oscillatory power may reflect a transient increase in granule cell excitability consistent with the data presented in Figure 5.

Increase in anxiety-like behaviors

Since the ventral hippocampus appears to play a role in anxiety-like behavior (Bannerman et al. 2003), we subjected mutants and controls to an elevated plus maze, an unfamiliar open field task, and the forced swim test to determine whether mossy cell degeneration affects locomotion and mood. In the acute phase after DT injection, mutants exhibit significantly more anxiety-like behaviors —such as spending less time in the open arm of the plus-maze (Figure 8A) or in the center arena of the open field (Figure S5A)—than DT-treated controls and mutants in the chronic phase, but show no difference in locomotor activity (Figure S5B–C). In the forced swim test, mutant animals during the acute phase spend less time immobile on Day 2 (Figure 8B), suggesting that they are hyper-reactive and more anxious about the water-swim stress. These results suggest that shortly after cell ablation causes mossy cell degeneration, granule-cell excitability increases, eliciting anxiety-like behaviors.

Impaired contextual discrimination

To address whether mossy cell degeneration leads to impaired hippocampus-dependent learning, we subjected DT-treated mutants and control littermates to two contextual discrimination paradigms. Mice in acute and chronic DT treatment phases were subjected to a one-trial contextual fear-conditioning test to assess whether, 3 hr and 24 hr after conditioning, mutants can discriminate shocking context A from a modality-different context B (Figure S5D). Whether in acute (Figure 8C) or chronic (Figure 8D) phases of DT-treatment, mutants and controls show similar freezing levels before and immediately after shock during conditioning, indicating mossy cell ablation has no impact on contextual fear

learning. On the recall test, however, mutant animals in the acute phase (but not chronic-phase mutants or controls) are unable to distinguish Context A from Context B 3 hr (genotype–context interaction $F(1,38)=3.1$, $p<0.05$; Newman–Keuls *post hoc* test, $p<0.05$ for control, $p=0.42$ for mutant) and 24 hr (Figure 8C) after conditioning. Notably, when mice are tested in the chronic phase of DT exposure, this impairment disappears both at 3 hr (context effect, $F(1,30)=24.1$, $p<0.01$; Newman–Keuls *post hoc* test, $p<0.005$ for control, $p<0.01$ for mutant) and 24 hr (Figure 8D) after conditioning. Contextual discrimination impairment in mutants therefore appears to occur only in the acute phase of DT exposure, when granule cell excitability is highest.

To investigate whether mutants' inability to discriminate contexts is consistent across tasks, we subjected naïve animals with acute DT exposure to a contextual step-through active avoidance task. In the initial latency test crossing from light to dark compartments, no difference was detected among genotypes before conditioning (42.4±11.3 s for control, 58.3±24.0 s for mutant, *t*-test, $p=0.54$). In Context X, mice entering the dark compartment received a single foot shock (0.12 mA, 2 s). Twenty-four hr after conditioning, the mice were placed back in the dark compartment, either in the non-shock Context Y or in the US-associated Context X (Figure S5E). Reverse latency to escape from the dark compartment (X or Y) was measured for each context. Control mice had longer escape latency from safe Context Y, while this was not seen in the mutants (Figure 8E). These results confirm that in the acute phase of mossy cell degeneration, mutants' recall for a fear memory in a specific context is impaired.

Finally, we used cued-fear conditioning (Figure 8F) and accelerating roratod task (Figure 8G) to confirm that behavioral deficits during the acute phase after DT treatment are restricted to hippocampal-dependent tasks. We saw no difference in performance in both tasks, suggesting that mossy cell degeneration has little or no effect on non-hippocampal tasks.

Discussion

This paper presents the first direct evidence that selective and extensive degeneration of dentate hilar mossy cells produces: 1) acute granule cell hyperexcitability, transient theta oscillation power enhancement, and transient impairment of contextual discrimination; 2) no epileptiform activity; 3) no reactive sprouting of mossy fibers; 4) reactive sprouting of inhibitory interneuronal axons in vacated IML.

Mossy cells inhibit dentate excitability

Many have investigated the question of whether, on balance, hilar mossy cells excite or inhibit granule cells (Sloviter 1991; Buckmaster and Schwartzkroin 1994; Ratzliff et al. 2004; Zappone and Sloviter 2004). *In vivo* stimulation of commissural fibers, including mossy cell axons, excites inhibitory interneurons (Buzsáki and Eidelberg 1982) that inhibit activity in dentate granule cells (Buzsáki and Eidelberg 1981; Douglas et al. 1983). Excitation of mossy cells *in vitro* slices excites granule cells weakly but inhibits granule cells disynaptically via excitation of inhibitory interneurons (Scharfman, 1995; Larimer and Strowbridge, 2008), a finding consistent with the earlier *in vivo* results.

Our demonstration that selective and extensive degeneration of mossy cells is followed by acute granule cell hyperexcitability provides direct evidence of mossy cells' net inhibitory role in the dentate gyrus. Our results also support the "dormant basket cell" hypothesis contention that mossy cell loss causes dentate granule cell hyperexcitability (Sloviter 1991). The robust decrease in sEPSC frequency in granule cells in our mutant line not only verifies ablation of excitatory inputs from mossy cells but also implies the lack of "irritable" mossy

cells even if as much as 10–20% of mutant mossy cells survive. Any granule cell hyperexcitability in our mutants after DT treatment is therefore unlikely to come from surviving “irritable” mossy cells. Since a single mossy cell may project to as many as 30,000 granule cells (Buckmaster and Jongen-Rêlo 1999), however, further study is warranted to find out how direct projection from mossy cells to granule cells affects dentate function.

How mossy cell loss induces granule cell hyperexcitability

During acute mossy cell degeneration, both excitatory and inhibitory inputs to individual granule cells decrease, yet granule cell hyperexcitability increases. Dentate granule cells are usually silent and fire rarely, except when the animal changes place field (Jung and McNaughton 1993; Leutgeb et al. 2007). This tonic inhibition of granule cell activity is mediated by action potential-dependent release of GABA from surrounding interneurons (Glykys and Mody 2007). Mossy cells under anesthesia, by contrast, fire at relatively high background firing rates (Henze and Buzsáki 2007), suggesting that excitatory projections from mossy cells to granule cells have minimal impact on overall granule cell activity. Since mossy cells do maintain hilar interneuronal activity, at least in part, however, any shut-down of mossy cell firing through degeneration should elicit strong di-synaptic disinhibition compared to conditions when hilar interneurons are simply lost. When the perforant path is stimulated (Figure 5), this decrease in inhibition at a single cell level could exceed the spike threshold of individual granule cells, resulting in an overall increase in the perforant path-evoked responses.

Mossy cell loss not implicated in limbic epilepsy

Even following mossy cell loss of 80–90% in the chronic post-DT phase, our subjects show no evidence of spontaneous epilepsy. Similarly, to post-ablation day 35 with dentate gyrus activity monitored 2–3 hr per day, mutants show no spontaneous seizure discharges, and with behavior monitored 8 hr per day, mutants display no spontaneous seizure-like behaviors. Because continuous 24 hr video recording is required to be definitive, however, we cannot exclude the possibility of sporadic seizures, and it is also possible that we saw no spontaneous seizures because not all of the mossy cells were completely degenerated. Our findings strongly suggest, however, that although mossy cell loss is associated with granule cell hyperexcitability, the loss of 80–90% of mossy cells alone is insufficient to cause spontaneous epilepsy.

It is plausible that to trigger dentate epileptogenesis, additional injuries or cellular deficits are needed, such as loss of both hilar interneurons and mossy cells (Sloviter 1987). The degree of hilar interneuron loss, however, appears to vary by epilepsy model and among patients (Ratzliff et al., 2002; Cossart et al., 2005), and in chronic epileptics, there is substantial evidence for compensatory sprouting of surviving interneurons (in animals, Davenport et al. 1990; Houser and Esclapez 1996; in humans, Mathern et al. 1995). These confounding factors make it difficult to determine exactly how hilar interneuronal loss and surviving interneurons affect dentate epileptogenesis (Cossart et al. 2005; Thind et al. 2010).

Temporal lobe epileptogenesis may also involve entorhinal cortex and other related structures. While granule cells may be powerful excitation amplifiers, we found that disinhibiting them cannot generate spontaneous epileptiform discharges without abnormal excitatory inputs from outside the hippocampus. Schwarcz and colleagues (Du et al. 1993) suggest that selective neuronal loss in the entorhinal cortex plays a pathophysiological role in epileptogenesis, a theory supported by recent studies (Bumanglag and Sloviter 2008). Generation of spontaneous epileptiform discharges, therefore, appears to require aberrant excitatory input from entorhinal cortex to disinhibited dentate granule cells.

Mossy cell loss elicits sprouting in interneuron axons but not in mossy fibers

Although it has been predicted that loss of the mossy cells that denervate the IML will trigger mossy fiber sprouting (Jiao and Nadler 2007), even 6–8 weeks after ~90% mossy cell ablation, we observed no mossy fiber sprouting. Rather, we saw delayed compensatory axon sprouting of GAD67-positive fibers—probably originating from inhibitory interneurons—into the IML. Concomitantly, the sIPSC frequency from the mutant granule cells, transiently decreased during the acute phase, returned to normal levels by the chronic phase, suggesting a slow process of synaptic reorganization to reverse acute granule cell hyperexcitability. In conclusion, mossy cell loss alone appears to be insufficient to trigger mossy fiber sprouting.

Mossy cell loss impairs contextual discrimination

Despite the lack of spontaneous seizure-like behaviors, massive mossy cell degeneration appears to hyperexcite dentate granule cells, impair contextual discrimination, and increase anxiety-like behavior. In a typical environment where granule cells are only rarely activated (Chawla et al. 2005), different incoming signals disperse onto largely non-overlapping granule cell populations, thereby supporting their role in pattern separation. In the acute phase of mossy cell degeneration, however, hyperexcitable granule cells tend to increase firing, which increases overlap and decreases pattern separation. Our findings suggest that mossy cells must maintain feed-forward inhibition of granule cell firing to achieve normal pattern separation. Anxiety-like behaviors during the acute phase of mossy cell degeneration may also be linked to dentate hyperexcitability in the ventral hippocampus.

Chronic mossy cell loss and dentate gyrus function

Our behavioral results during the chronic phase suggest that long-term mossy cell loss *per se* has little effect on the anxiety-like behavior and contextual discrimination tasks we assessed. One possible explanation is that inhibitory axonal sprouting onto granule cells during the chronic phase may restore a low rate of granule cell firing and thereby restore the network. Whereas the activation of mature granule cells is limited by such inhibition, the impact on immature granule cells, whose activation threshold and input specificity are low (Marín-Burgin et al. 2012), may alter behavior. However, since we see no difference between chronic phase DT-treated mutants and controls in number of doublecortin-positive cells and proliferating cell-nuclear antigen (PCNA)-positive cells at the subgranular layer, it appears that mossy cell loss has no detectable impact on adult neurogenesis (Jinde et al., unpublished result). Nevertheless, without mossy cell feed-forward excitation of hilar interneurons, excitation of dentate interneurons (by perforant path, granule cells, or CA3 pyramidal cells) may not be strong enough to inhibit granule cells (Sloviter 1991). It is therefore possible that more complex tasks or perturbations could reveal selective deficits in mutant mice, even in the chronic phase.

In sum, our findings regarding the *in vivo* function of hilar mossy cells indicate that they play a pivotal role in the inhibition of dentate excitability to maintain the pattern separation function among granule cells. We further show that, despite increased excitability following massive but selective mossy cell degeneration, no epileptogenic signs occur, suggesting that hilar interneurons or other limbic areas (such as entorhinal cortex) may be more important for limbic seizure generation. Finally, our genetically engineered mossy cell-restricted mice offer opportunities for future studies of the mossy cell function at the cellular, network, and system levels.

Experimental Procedures

All experiments were carried out in accordance with the National Research Council's Guide for the Care and Use of Laboratory Animals and approved by the NIMH Animal Care and Use Committee. For detailed experimental procedures, see Supplemental Information.

The Mossy Cell-Restricted Inducible Cell Ablation Mutant Mouse

To generate mossy cell/CA3-Cre lines, a DNA fragment containing the 5′-transcriptional regulatory region of the murine calcitonin receptor-like receptor (*Crlr*) was co-injected with Cre recombinase cDNA carrying HSP70 minimal promoter into pronuclei of C57BL/6 mouse eggs. We also generated *loxP*-flanked diphtheria toxin receptor (fDTR) transgenic lines in which a Cre-mediated recombination human heparin-binding epidermal growth factor–like growth factor (HB-EGF, I117V/L148V mutant, see Furukawa et al. 2006) was expressed under the control of the murine CaMKIIα promoter. To generate inducible mossy cell ablation mutant mice, we intercrossed a mossy cell/CA3-Cre line (#4688) with a fDTR (line-B), thus generating mutant mice (Cre +/−; fDTR +/−) and three control littermates (hemizygous fDTR-line B, hemizygous-Cre, and wild-type) mice. Between 8–20 weeks of age, all groups were treated with diphtheria toxin (DT, Sigma D0564; *i.p.* injection at 25μg/kg per day) or saline for 2 consecutive days.

Slice Physiology

Whole-cell recordings were made from dentate granule cells of the mutant mouse line and their littermates (aged 12–20 weeks) under an upright microscope with DIC/infrared/fluorescence optics (Olympus) as described in Belforte et al. (2010).

In Vivo Physiology

LFP recordings were conducted using a microwire array consisting of seven Formvar-insulated nichrome wires aligned in a single slanted row to vary the depth of recording, with an inter-electrode separation of 50–100 μm, as described in Jinde et al. (2009) with modifications. Power spectrogram distribution of dentate LFPs was averaged in periods of exploration and immobility as estimated by animal head movement.

Behavioral Tests for Contextual Discrimination

Mouse experimental groups included an *acute-phase* (5–7 days after DT treatment, n=22 mutant; n=20 control) and a separate *chronic phase* (4–6 weeks after treatment, n=16 mutant; n=16 control) cohort, which were subjected to one-trial contextual fear conditioning to assess pattern separation, as described in Cravens et al. (2006). Naïve acute phase mutants (n=8) and controls (n=9) were also subjected to a one-trial contextual active avoidance task, as described in Cravens et al. (2006).

Statistical Comparisons

Results are reported as mean ± SEM. Comparisons were made with Student's *t*-test for equal means, unless otherwise specified.

Supplementary Material

Refer to Web version on PubMed Central for supplementary material.

Acknowledgments

We thank RS Sloviter for discussions and helpful comments on the manuscript. We also thank RD Palmiter for a gift of anti-ZnT3, S Itohara for anti-Netrin G2, NM Vargas-Pinto, ER Sklar, and S Zhang for technical assistance,

and S Kolata and E Sherman for critical reading of the manuscript. This research was supported by the Intramural Research Programs of the NIMH. This research was partially supported by a Grant-in-Aid for Scientific Research of Ministry of Education, Culture, Sports, Science and Technology, Japan (Grant #: 22591274). SJ was supported by a Japan Society for the Promotion of Science (JSPS) fellowship.

Abbreviations

CR	calretinin, ventral mossy cell marker
Ctl	control
Cx	cerebral cortex
DG	dentate gyrus
DGC	dentate granule cell
DT	diphtheria toxin
GluA2/3	mossy cell marker in hilar region
IML	inner molecular layer
MF	mossy fiber
Mut	mutant
NPY	Neuropeptide Y, hilar interneuron marker
OML	outer molecular layer
ST	striatum
TH	thalamus
vHP	ventral hippocampus

References

Amaral DG. A Golgi study of cell types in the hilar region of the hippocampus in the rat. J Comp Neurol. 1978; 182:851–914. [PubMed: 730852]

Amaral DG, Witter MP. The three-dimensional organization of the hippocampal formation: a review of anatomical data. Neuroscience. 1989; 31:571–591. [PubMed: 2687721]

Bannerman DM, Grubb M, Deacon RM, Yee BK, Feldon J, Rawlins JN. Ventral hippocampal lesions affect anxiety but not spatial learning. Behav Brain Res. 2003; 139:197–213. [PubMed: 12642189]

Belforte JE, Zsiros V, Sklar ER, Jiang Z, Yu G, Li Y, Quinlan EM, Nakazawa K. Postnatal NMDA receptor ablation in corticolimbic interneurons confers schizophrenia-like phenotypes. Nat Neurosci. 2010; 13:76–83. [PubMed: 19915563]

Bilkey DK, Goddard GV. Septohippocampal and commissural pathways antagonistically control inhibitory interneurons in the dentate gyrus. Brain Res. 1987; 405:320–325. [PubMed: 3567610]

Blackstad TW. Commissural connections of the hippocampal region in the rat, with special reference to their mode of termination. J Comp Neurol. 1956; 105:417–537. [PubMed: 13385382]

Blümcke I, Suter B, Behle K, Kuhn R, Schramm J, Elger CE, Wiestler OD. Loss of hilar mossy cells in Ammon's horn sclerosis. Epilepsia. 2000; 41(Suppl 6):S174–S180. [PubMed: 10999540]

Bragin A, Jandó G, Nádasdy Z, Hetke J, Wise K, Buzsáki G. Gamma (40–100 Hz) oscillation in the hippocampus of the behaving rat. J Neurosci. 1995a; 15:47–60. [PubMed: 7823151]

Bragin A, Jandó G, Nádasdy Z, van Landeghem M, Buzsáki G. Dentate EEG spikes and associated interneuronal population bursts in the hippocampal hilar region of the rat. J Neurophysiol. 1995b; 73:1691–1705. [PubMed: 7643175]

Buckmaster PS, Jongen-Rêlo AL. Highly specific neuron loss preserves lateral inhibitory circuits in the dentate gyrus of kainate-induced epileptic rats. J Neurosci. 1999; 19:9519–9529. [PubMed: 10531454]

Buckmaster PS, Schwartzkroin PA. Hippocampal mossy cell function: a speculative view. Hippocampus. 1994; 4:393–402. [PubMed: 7874231]

Buckmaster PS, Strowbridge BW, Kunkel DD, Schmiege DL, Schwartzkroin PA. Mossy cell axonal projections to the dentate gyrus molecular layer in the rat hippocampal slice. Hippocampus. 1992; 2:349–362. [PubMed: 1284975]

Buckmaster PS, Wenzel HJ, Kunkel DD, Schwartzkroin PA. Axon arbors and synaptic connections of hippocampal mossy cells in the rat *in vivo*. J Comp Neurol. 1996; 366:271–292. [PubMed: 8698887]

Bumanglag AV, Sloviter RS. Minimal latency to hippocampal epileptogenesis and clinical epilepsy after perforant pathway stimulation-induced status epilepticus in awake rats. J Comp Neurol. 2008; 510:561–580. [PubMed: 18697194]

Buzsáki G, Eidelberg E. Commissural projection to the dentate gyrus of the rat: evidence for feed-forward inhibition. Brain Res. 1981; 230:346–350. [PubMed: 7317783]

Buzsáki G, Eidelberg E. Direct afferent excitation and long-term potentiation of hippocampal interneurons. J Neurophysiol. 1982; 48:597–607. [PubMed: 6290613]

Chawla MK, Guzowski JF, Ramirez-Amaya V, Lipa P, Hoffman KL, Marriott LK, Worley PF, McNaughton BL, Barnes CA. Sparse, environmentally selective expression of Arc RNA in the upper blade of the rodent fascia dentata by brief spatial experience. Hippocampus. 2005; 15:579–586. [PubMed: 15920719]

Corbetta S, Gualdoni S, Ciceri G, Monari M, Zuccaro E, Tybulewicz VLJ, de Curtis I. Essential role of Rac1 and Rac3 GTPases in neuronal development. FASEB J. 2009; 23:1347–1357. [PubMed: 19126596]

Cossart R, Bernard C, Ben-Ari Y. Multiple facets of GABAergic neurons and synapses: multiple fates of GABA signalling in epilepsies. Trends Neurosci. 2005; 28:108–115. [PubMed: 15667934]

Cravens CJ, Vargas-Pinto N, Christian KM, Nakazawa K. CA3 NMDA receptors are crucial for rapid and automatic representation of context memory. Eur J Neurosci. 2006; 24:1771–1780. [PubMed: 17004940]

Davenport CJ, Brown WJ, Babb TL. Sprouting of GABAergic and mossy fiber axons in dentate gyrus following intrahippocampal kainate in the rat. Exp Neurol. 1990; 109:180–190. [PubMed: 1696207]

Deller T, Nitsch R, Frotscher M. Associational and commissural afferents of parvalbumin-immunoreactive neurons in the rat hippocampus: a combined immunocytochemical and PHA-L study. J Comp Neurol. 1994; 350:612–622. [PubMed: 7890833]

Douglas RM, McNaughton BL, Goddard GV. Commissural inhibition and facilitation of granule cell discharge in fascia dentata. J Comp Neurol. 1983; 219:285–294. [PubMed: 6311879]

Du F, Whetsell WO Jr, Abou-Khalil B, Blumenköpf B, Lothman EW, Schwarcz R. Preferential neuronal loss in layer III of the entorhinal cortex in patients with temporal lobe epilepsy. Epilepsy Res. 1993; 16:223–233. [PubMed: 8119273]

Frotscher M, Seress L, Schwerdtfeger WK, Buhl E. The mossy cells of the fascia dentata: a comparative study of their fine structure and synaptic connections in rodents and primates. J Comp Neurol. 1991; 312:145–163. [PubMed: 1744242]

Fujise N, Liu Y, Hori N, Kosaka T. Distribution of calretinin immunoreactivity in the mouse dentate gyrus: II. Mossy cells, with special reference to their dorsoventral difference in calretinin immunoreactivity. Neuroscience. 1998; 82:181–200. [PubMed: 9483514]

Furukawa N, Saito M, Hakoshima T, Kohno K. A diphtheria toxin receptor deficient in epidermal growth factor-like biological activity. J Biochem. 2006; 140:831–841. [PubMed: 17071947]

Glykys J, Mody I. The main source of ambient GABA responsible for tonic inhibition in the mouse hippocampus. J Physiol. 2007; 582:1163–1178. [PubMed: 17525114]

Henze DA, Buzsáki G. Hilar mossy cells: functional identification and activity *in vivo*. Prog Brain Res. 2007; 163:199–216. [PubMed: 17765720]

Houser CR, Esclapez M. Vulnerability and plasticity of the GABA system in the pilocarpine model of spontaneous recurrent seizures. Epilepsy Res. 1996; 26:207–218. [PubMed: 8985701]

Hsu M, Buzsáki G. Vulnerability of mossy fiber targets in the rat hippocampus to forebrain ischemia. J Neurosci. 1993; 13:3964–3979. [PubMed: 8366355]

Jiao Y, Nadler JV. Stereological analysis of GluR2-immunoreactive hilar neurons in the pilocarpine model of temporal lobe epilepsy: correlation of cell loss with mossy fiber sprouting. Exp Neurol. 2007; 205:569–582. [PubMed: 17475251]

Jinde S, Belforte JE, Yamamoto J, Wilson MA, Tonegawa S, Nakazawa K. Lack of kainic acid-induced gamma oscillations predicts subsequent CA1 excitotoxic cell death. Eur J Neurosci. 2009; 30:1036–1055. [PubMed: 19735292]

Johansen FF, Zimmer J, Diemer NH. Early loss of somatostatin neurons in dentate hilus after cerebral ischemia in the rat precedes CA-1 pyramidal cell loss. Acta Neuropathol. 1987; 73:110–114. [PubMed: 2885998]

Jung MW, McNaughton BL. Spatial selectivity of unit activity in the hippocampal granular layer. Hippocampus. 1993; 3:165–182. [PubMed: 8353604]

Kienzler F, Norwood BA, Sloviter RS. Hippocampal injury, atrophy, synaptic reorganization, and epileptogenesis after perforant pathway stimulation-induced status epilepticus in the mouse. J Comp Neurol. 2009; 515:181–196. [PubMed: 19412934]

Kocsis B, Bragin A, Buzsáki G. Interdependence of multiple theta generators in the hippocampus: a partial coherence analysis. J Neurosci. 1999; 19:6200–6212. [PubMed: 10407056]

Larimer P, Strowbridge BW. Nonrandom local circuits in the dentate gyrus. J Neurosci. 2008; 28:12212–12223. [PubMed: 19020015]

Leranth C, Szeidemann Z, Hsu M, Buzsáki G. AMPA receptors in the rat and primate hippocampus: a possible absence of GluR2/3 subunits in most interneurons. Neuroscience. 1996; 70:631–652. [PubMed: 9045077]

Leutgeb JK, Leutgeb S, Moser MB, Moser EI. Pattern separation in the dentate gyrus and CA3 of the hippocampus. Science. 2007; 315:961–966. [PubMed: 17303747]

Liu Y, Fujise N, Kosaka T. Distribution of calretinin immunoreactivity in the mouse dentate gyrus. I General description. Exp Brain Res. 1996; 108:389–403. [PubMed: 8801119]

Lowenstein DH, Thomas MJ, Smith DH, McIntosh TK. Selective vulnerability of dentate hilar neurons following traumatic brain injury: a potential mechanistic link between head trauma and disorders of the hippocampus. J Neurosci. 1992; 12:4846–4853. [PubMed: 1464770]

Lübke J, Deller T, Frotscher M. Septal innervation of mossy cells in the hilus of the rat dentate gyrus: an anterograde tracing and intracellular labeling study. Exp Brain Res. 1997; 114:423–432. [PubMed: 9187278]

Margerison JH, Corsellis JA. Epilepsy and the temporal lobes. A clinical, electroencephalographic and neuropathological study of the brain in epilepsy, with particular reference to the temporal lobes. Brain. 1966; 89:499–530. [PubMed: 5922048]

Marín-Burgin A, Mongiat LA, Pardi MB, Schinder AF. Unique processing during a period of high excitation/inhibition balance in adult-born neurons. Science. 2012; 335:1238–1242. [PubMed: 22282476]

Mathern GW, Babb TL, Pretorius JK, Leite JP. Reactive synaptogenesis and neuron densities for neuropeptide Y, somatostatin, and glutamate decarboxylase immunoreactivity in the epileptogenic human fascia dentata. J Neurosci. 1995; 15:3990–4004. [PubMed: 7751960]

Myers CE, Scharfman HE. A role for hilar cells in pattern separation in the dentate gyrus: a computational approach. Hippocampus. 2009; 19:321–337. [PubMed: 18958849]

Nishimura-Akiyoshi S, Niimi K, Nakashiba T, Itohara S. Axonal netrin-Gs transneuronally determine lamina-specific subdendritic segments. Proc Natl Acad Sci USA. 2007; 104:14801–14806. [PubMed: 17785411]

Ratzliff AH, Santhakumar V, Howard A, Soltesz I. Mossy cells in epilepsy: rigor mortis or vigor mortis? Trends Neurosci. 2002; 25:140–144. [PubMed: 11852145]

Ratzliff AH, Howard AL, Santhakumar V, Osapay I, Soltesz I. Rapid deletion of mossy cells does not result in a hyperexcitable dentate gyrus: implications for epileptogenesis. J Neurosci. 2004; 24:2259–2269. [PubMed: 14999076]

Saito M, Iwawaki T, Taya C, Yonekawa H, Noda M, Inui Y, Mekada E, Kimata Y, Tsuru A, Kohno K. Diphtheria toxin receptor-mediated conditional and targeted cell ablation in transgenic mice. Nat Biotechnol. 2001; 19:746–750. [PubMed: 11479567]

Santhakumar V, Bender R, Frotscher M, Ross ST, Hollrigel GS, Toth Z, Soltesz I. Granule cell hyperexcitability in the early post-traumatic rat dentate gyrus: the 'irritable mossy cell' hypothesis. J Physiol. 2000; 524:117–134. [PubMed: 10747187]

Santhakumar V, Ratzliff AD, Jeng J, Toth K, Soltesz I. Long-term hyperexcitability in the hippocampus after experimental head trauma. Ann Neurol. 2001; 50:708–717. [PubMed: 11761468]

Scharfman HE. Electrophysiological evidence that dentate hilar mossy cells are excitatory and innervate both granule cells and interneurons. J Neurophysiol. 1995; 74:179–194. [PubMed: 7472322]

Scharfman HE. The CA3 "backprojection" to the dentate gyrus. Prog Brain Res. 2007; 163:627–637. [PubMed: 17765742]

Scharfman HE, Schwartzkroin PA. Electrophysiology of morphologically identified mossy cells of the dentate hilus recorded in guinea pig hippocampal slices. J Neurosci. 1988; 8:3812–3821. [PubMed: 2461436]

Schmued LC, Hopkins KJ. Fluoro-Jade B: a high affinity fluorescent marker for the localization of neuronal degeneration. Brain Res. 2000; 874:123–130. [PubMed: 10960596]

Seress L, Ribak CE. Direct commissural connections to the basket cells of the hippocampal dentate gyrus: anatomical evidence for feedforward inhibition. J Neurocytol. 1984; 13:215–225. [PubMed: 6726288]

Sloviter RS. "Epileptic" brain damage in rats induced by sustained electrical stimulation of the perforant path. I Acute electrophysiological and light microscopic studies. Brain Res Bull. 1983; 10:675–697. [PubMed: 6871737]

Sloviter RS. Decreased hippocampal inhibition and a selective loss of interneurons in experimental epilepsy. Science. 1987; 235:73–76. [PubMed: 2879352]

Sloviter RS. Permanently altered hippocampal structure, excitability, and inhibition after experimental status epilepticus in the rat: the "dormant basket cell" hypothesis and its possible relevance to temporal lobe epilepsy. Hippocampus. 1991; 1:41–66. [PubMed: 1688284]

Sloviter RS, Zappone CA, Harvey BD, Bumanglag AV, Bender RA, Frotscher M. "Dormant basket cell" hypothesis revisited: relative vulnerabilities of dentate gyrus mossy cells and inhibitory interneurons after hippocampal status epilepticus in the rat. J Comp Neurol. 2003; 459:44–76. [PubMed: 12629666]

Soriano E, Frotscher M. Mossy cells of the rat fascia dentata are glutamate-immunoreactive. Hippocampus. 1994; 4:65–69. [PubMed: 7914798]

Tauck DL, Nadler JV. Evidence of functional mossy fibre sprouting in hippocampal formation of kainic acid-treated rats. J Neurosci. 1985; 5:1016–1022. [PubMed: 3981241]

Thind KK, Yamawaki R, Phanwar I, Zhang G, Wen X, Buckmaster PS. Initial loss but later excess of GABAergic synapses with dentate granule cells in a rat model of temporal lobe epilepsy. J Comp Neurol. 2010; 518:647–667. [PubMed: 20034063]

Toth Z, Hollrigel GS, Gorcs T, Soltesz I. Instantaneous perturbation of dentate interneuronal networks by a pressure wave-transient delivered to the neocortex. J Neurosci. 1997; 17:8106–8117. [PubMed: 9334386]

Wenzel HJ, Buckmaster PS, Anderson NL, Wenzel ME, Schwartzkroin PA. Ultrastructural localization of neurotransmitter immunoreactivity in mossy cell axons and their synaptic targets in the rat dentate gyrus. Hippocampus. 1997; 7:559–570. [PubMed: 9347352]

West MJ, Andersen AH. An allometric study of the area dentate in rat and mouse. Brain Res Rev. 1980; 2:317–348.

Williams PA, Larimer P, Gao Y, Strowbridge BW. Semilunar granule cells: glutamatergic neurons in the rat dentate gyrus with axon collaterals in the inner molecular layer. J Neurosci. 2007; 27:13756–13761. [PubMed: 18077687]

Wittner L, Henze DA, Záborszky L, Buzsáki G. Three-dimensional reconstruction of the axon arbor of a CA3 pyramidal cell recorded and filled *in vivo*. Brain Struct Funct. 2007; 212:75–83. [PubMed: 17717699]

Zappone CA, Sloviter RS. Commissurally projecting inhibitory interneurons of the rat hippocampal dentate gyrus: a colocalization study of neuronal markers and the retrograde tracer Fluoro-gold. J Comp Neurol. 2001; 441:324–344. [PubMed: 11745653]

Zappone CA, Sloviter RS. Translamellar disinhibition in the rat hippocampal dentate gyrus after seizure-induced degeneration of vulnerable hilar neurons. J Neurosci. 2004; 24:853–864. [PubMed: 14749430]

Highlights

1. New transgenic mouse line with inducible rapid degeneration of mossy cells.
2. Interneurons driven by mossy cells inhibit granule cell activity.
3. Loss of mossy cells alone is insufficient to trigger limbic epileptogenesis.
4. Mossy cell control of dentate excitability affects pattern separation function.

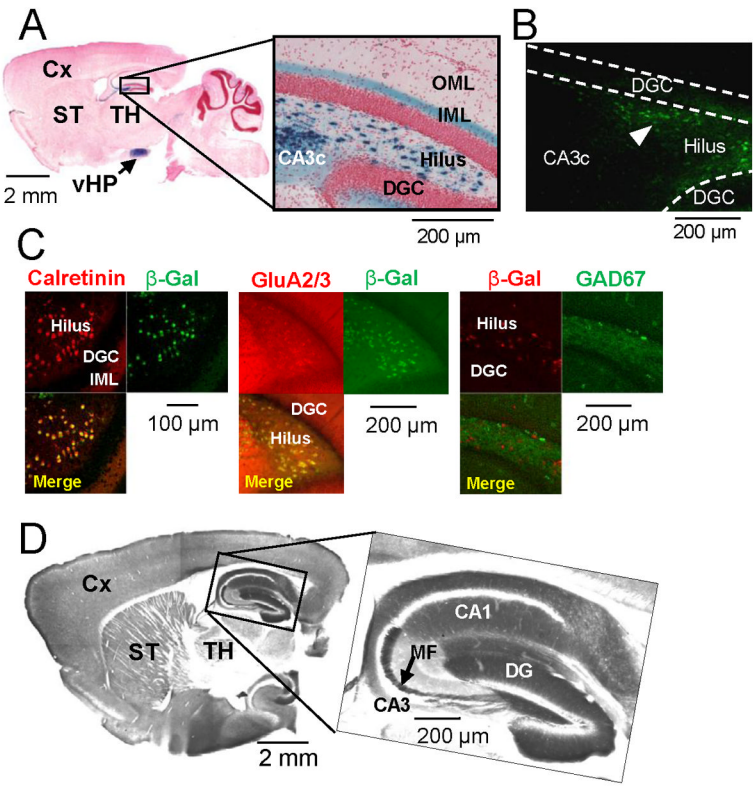

Figure 1. Generation and characterization of Cre and floxed-diphtheria toxin receptor lines

(A–C) Generation of mossy cell/CA3-Cre transgenic line #4688. (A) A parasagittal section stained with X-gal and Safranin O from the brain of Cre mice crossed with *loxP*-flanked Rosa26*LacZ* (8-wk old) reporter line (arrow, ventral hippocampus). (B) Cre-IR in the dentate gyrus of (8-wk old) Cre mice. Note that Cre is expressed selectively in the dentate hilus (arrowhead) but not in area CA3c. (C) Confocal immunostaining images of β-gal (green, recombination product) with calretinin (red, mossy cell marker) or GluA2/3 (red, mossy cell marker), and β-gal (red) with GAD67 (green, GABAergic interneuron marker), of Cre/Rosa26*LacZ* double transgenic mouse show more than 90% of calretinin- or GluA2/3-positive cells are β-gal positive but no colocalization of β-gal with GAD67. (D) Alkaline phosphatase-stained parasagittal section from the brain of (8-wk old) floxed-diphtheria toxin receptor (fDTR) line-B.

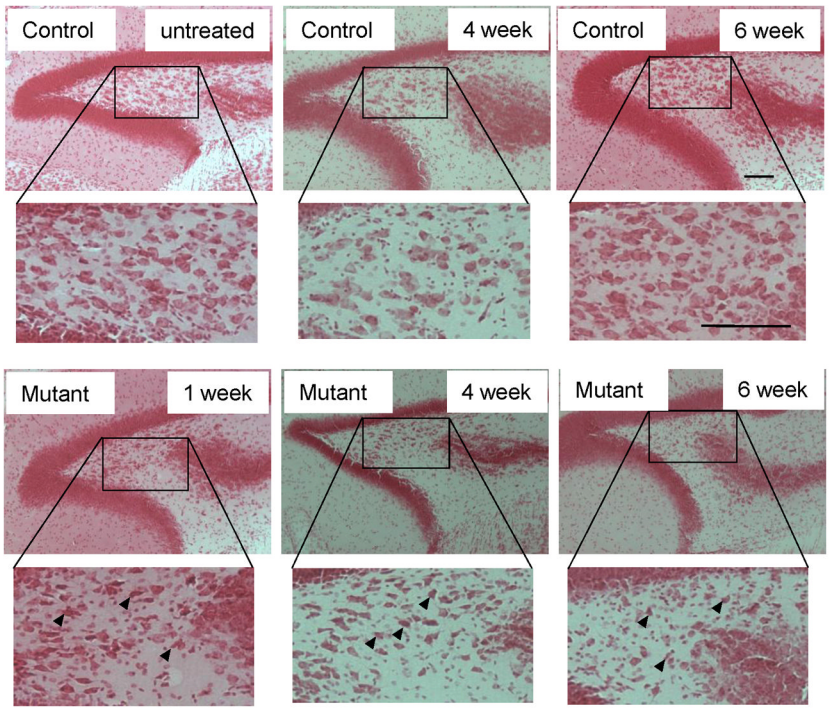

Figure 2. Time course of mossy cell degeneration

Representative photographs of Nissl staining after diphtheria toxin (DT) administration show histological alterations in the hilar region in mutant mice (n=3 for each genotype) compared to saline- or DT-treated controls. Cellular condensation with pyknotic nuclei (arrowheads) is prominent from post-DT day 7 and more severe 4 and 6 weeks after DT treatment, and increased extra-neuronal space suggests swollen investing glial cells. Scale bar, 100 μm.

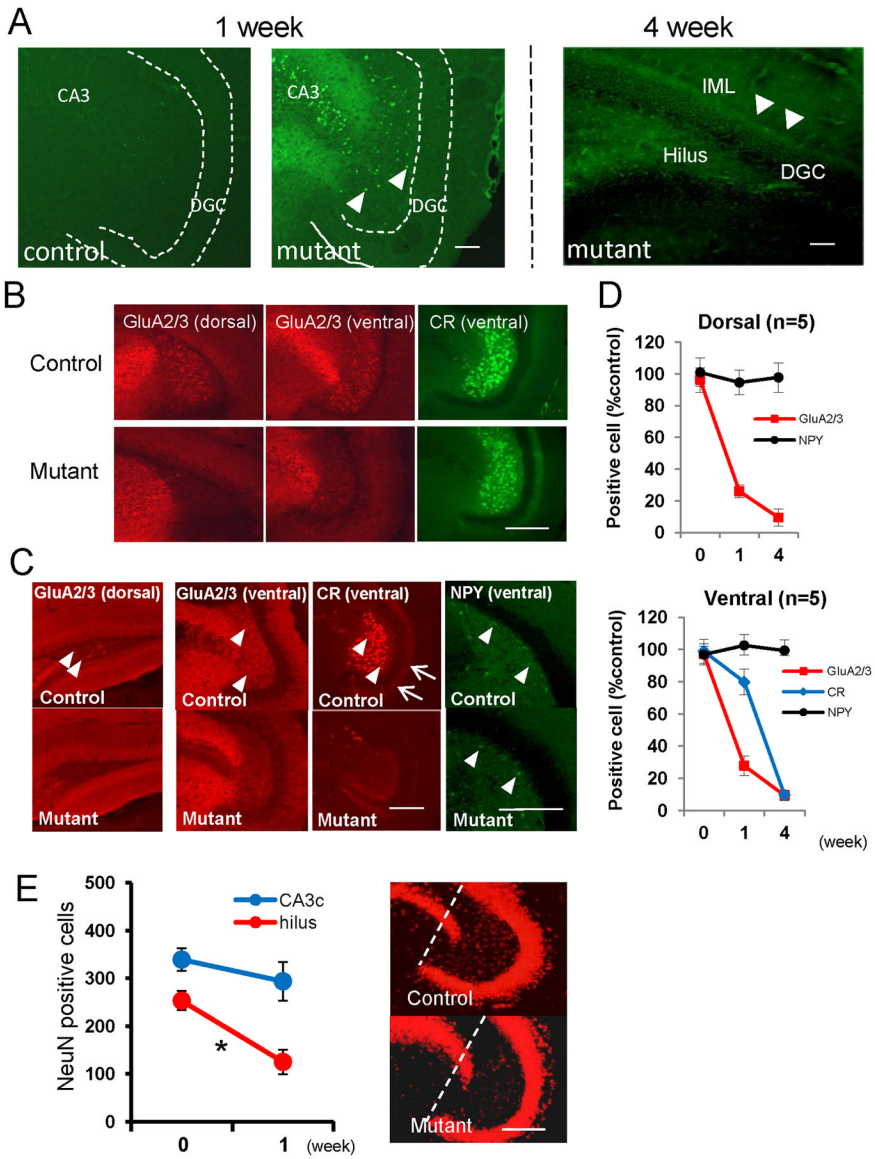

Figure 3. Massive neurodegeneration of mossy cells in Cre/fDTR mutants after diphtheria toxin treatment

(A) *Fluoro-Jade B (FJB) staining of mutant mouse after DT treatment.* Week 1: FJB-positive cells in area CA3 and dentate hilus (arrowheads) in mutants but not in DT-treated controls. Week 4: FJB-positive cell somata disappear in the hilus. Degenerated fibers in dentate hilus and IML are stained (right).

(B) *Acute phase staining of mossy cell markers (1 week post-DT).* Representative images of immunostained sections from same animal brain. Note hilar cells no longer positive for anti-GluA2/3 but ventral hilar cells still largely positive for anti-calretinin (CR).

(C) *Chronic phase cell marker staining (4 weeks post-DT).* Immuno-positive cells for GluA2/3 (in both dorsal and ventral hippocampi) and for calretinin are reduced in mutant mice compared to control mice, with no difference in cell numbers positive for neuropeptide Y (NPY). Arrowheads: immune-positive cells for each marker in the hilus; Arrows: CR-positive mossy cell axons in IML.

(D) Number of immuno-positive cells for each marker over time in mutants (compared to controls as 100%): immediately (n=5), 1 wk (n=5), and 4 wk (n=5) post-DT.
(E) *NeuN-positive neurons in area CA3c and hilar region of the ventral hippocampus before and 1 wk after DT treatment.* Area CA3c is between the dentate gyrus blades (see dotted lines). After DT treatment, the number of NeuN-positive neurons in the CA3c layer of mutant (n=4) does not differ significantly from that in DT-treated controls (n=4) but is robustly reduced in the mutant hilar regions, suggesting that DT affects CA3c pyramidal neurons only minimally. *t*-test for CA3c pyramidal neurons ($p=0.37$) and for hilar neurons ($*p<0.01$). Scale bar, 100 μm.

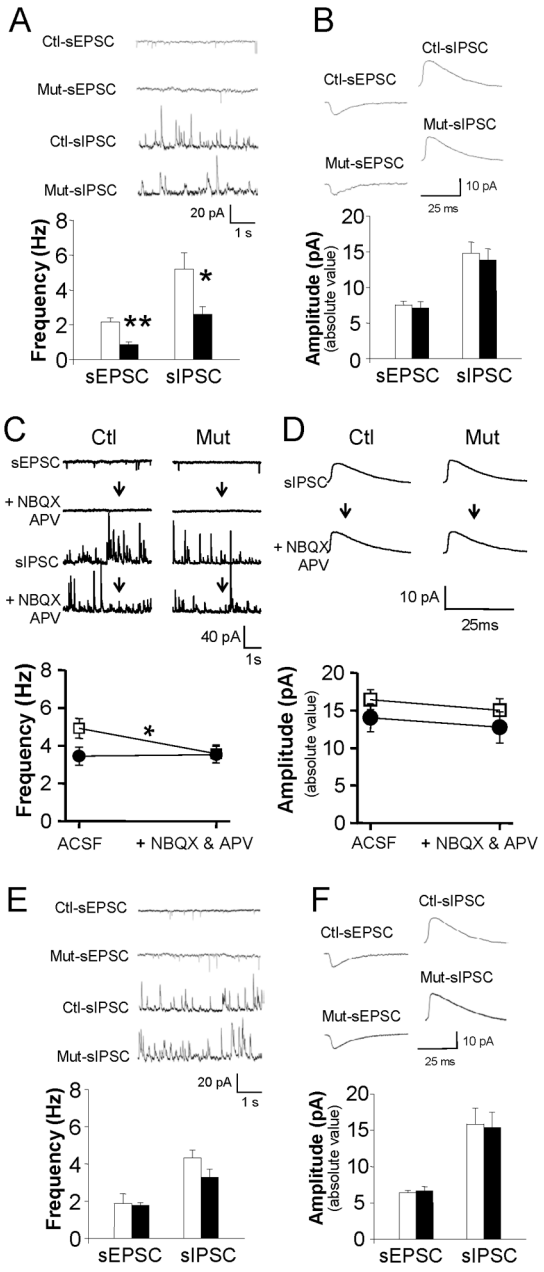

Figure 4. Acute mossy cell degeneration decreases excitatory and inhibitory inputs to granule cells

(A–B) Decreases in sEPSCs and sIPSCs frequency in dentate granule cells during the acute phase (post-DT 4–11 days) suggest that granule cells normally receive both excitatory inputs from mossy cells directly and disynaptic inhibitory inputs from mossy cells indirectly via local interneurons. *t*-test (**$p<0.001$, *$p<0.03$).

(C–D) *Mossy cell synaptic inhibition lost during the acute phase.* Changes in the sEPSC frequency show that NBQX and APV abolish glutamatergic transmission. That blockade of glutamatergic transmission reduces sIPSC frequency in control slices (n=10) but not in mutants (n=6) suggests that mossy cells mediate ipsilateral feed-forward inhibition. Blockade of glutamatergic transmission does not affect sEPSC amplitudes (p=0.366). □ = control; ● = mutant (*$p< 0.05$).

(E–F) *sEPSC and sIPSC in dentate granule cells during the chronic phase*. DT-mediated mossy cell ablation does not appear to affect the frequency or amplitude of sEPSC and sIPSC events. *Insets:* 5-s long continuous (upper left) and averaged (upper right) recordings of sEPSC and sIPSC events in chronic controls (n=8) and mutants (n=7).

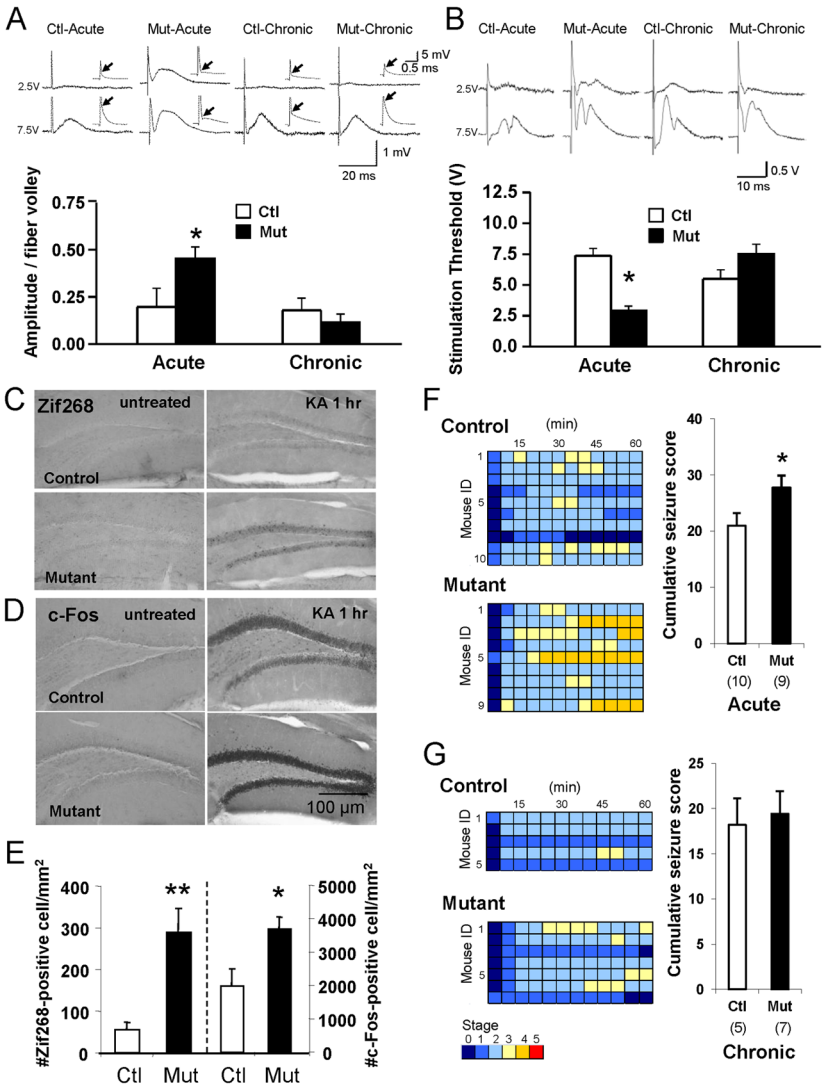

Figure 5. Transient increase in dentate excitability in acute phase

(A) *Evoked fEPSP amplitudes on perforant path show transient increase in excitability in DT-treated mutants. Insets*: fEPSPs generated with 2.5 V *(upper)* and 7.5 V *(lower)* stimulation intensities. A linear curve was fit to at least two data points per slice. Mean values from slices calculated for both controls (n=6) and mutants (n=7) in both the acute and chronic phase post-DT were averaged per animal to calculate mean amplitude/fiber volley. Arrows: location of fiber volley.

(B) *Mossy cell ablation transiently decreases population spike threshold in mutants. Insets*: 0.05 ms stimuli with intensities of 2.5V (upper) and 7.5V (lower). Stimulation threshold is minimum intensity (1, 2.5, 5, 7.5, or 10 V) needed to evoke high-fidelity population spikes. When no population spikes were evoked at 10 V, the threshold was arbitrarily set at 12.5 V. Acute control (n=7), acute mutant (n=9), chronic control (n=8), chronic mutant (n=8).

(C–E) *Immediate early gene expression increases after KA treatment in mutants.* (C) Representative photomicrographs of granule cells' Zif268 expression in acute phase *(upper)* controls (Racine scale seizure score = 3) and *(lower)* mutants (seizure score = 4) untreated *(left)* and 1 hr after KA treatment (*right*, 20mg/kg, *i.p.*). (D) c-Fos in *(upper)* controls and *(lower)* mutants, *(left)* untreated and *(right)* 1 hr after KA treatment (20mg/kg, *i.p.*). (E)

Acute phase, KA-induced expression of Zif268 and c-Fos is much more robust in mutants (n=8) than in controls (n=8). *t*-test (**p*<0.05, ***p*<0.01).
(F–G) *Mutants more susceptible to KA-induced seizures during acute phase but not in chronic phase.* (F) *(Left)* Time course of seizure severity following KA treatment (20 mg/kg, *i.p.*) in acute phase *(lower)* mutants and *(upper)* controls. Each animal's maximum seizure score was measured every 5 min over a 2-hr period. Timescale in one box is 5 min. *(Right)* Columns represent the cumulative seizure score measured over a 1-hr period after KA injection. *t*-test (**p*<0.05). Number in parentheses indicates number of animals. Note that KA-induced seizures are more severe in mutant mice than in controls. (G) *(Left)* Time course of seizure severity following KA treatment (20 mg/kg, *i.p.*) in chronic phase *(lower)* mutants and *(upper)* controls. Otherwise same as Figure 5F. *(Right)* Cumulative seizure scores are the same in mutants and controls in the chronic phase.

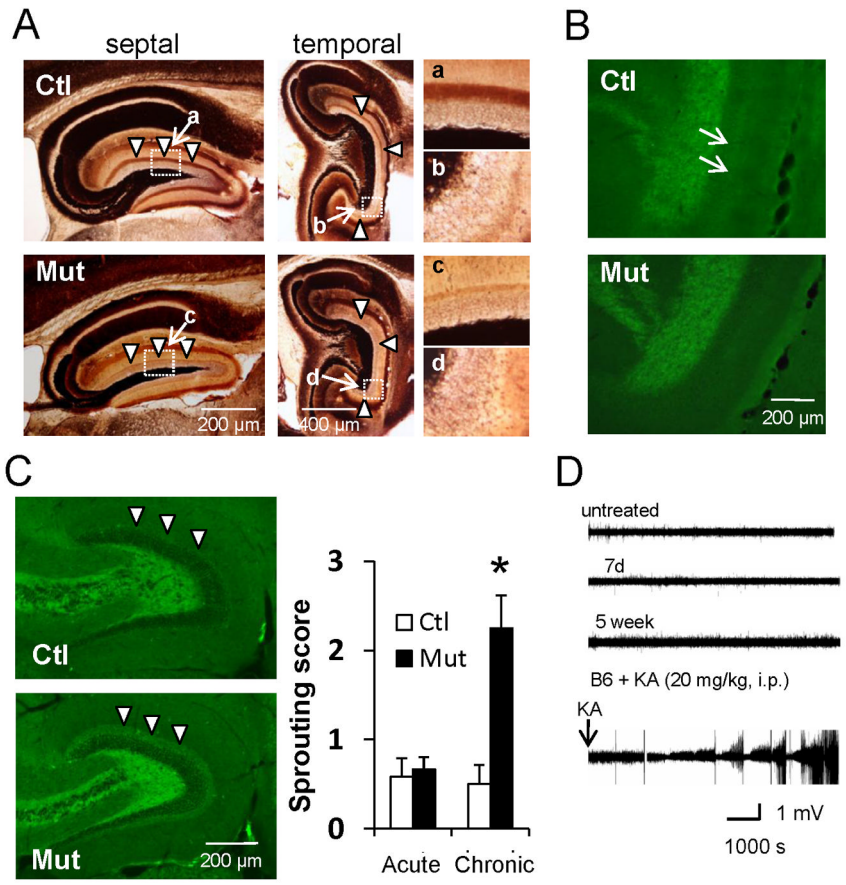

Figure 6. Functional changes after mossy cell loss

(A) *Timm staining of septal and temporal hippocampi during the chronic phase after mossy cell loss.* Mutants show no mossy fiber sprouting and mossy cell axon terminal band-like staining in IML (arrowheads) almost disappears.

(B) ZnT3-IR in mutants shows no mossy fiber sprouting and loss of mossy cell axon terminal band-like staining in IML (see arrows in control).

(C) *(Left*) Hippocampal GAD67-IR during chronic phase. *(Right)* The sprouting score (modified Tauck and Nadler method) is higher in mutant IML than in controls (arrowheads). Mann-Whitney *U*-test (**p*<0.05).

(D) Representative 2 hr traces of *in vivo* LFP recorded from mutant mouse before treatment *(untreated)* and 7 days *(acute phase)* and 5 weeks *(chronic phase)* after DT treatment. Epileptic LFP events following KA injection (20 mg/kg *i.p.*) to wild-type mouse are also shown. No obvious epileptiform discharges were observed following DT treatment.

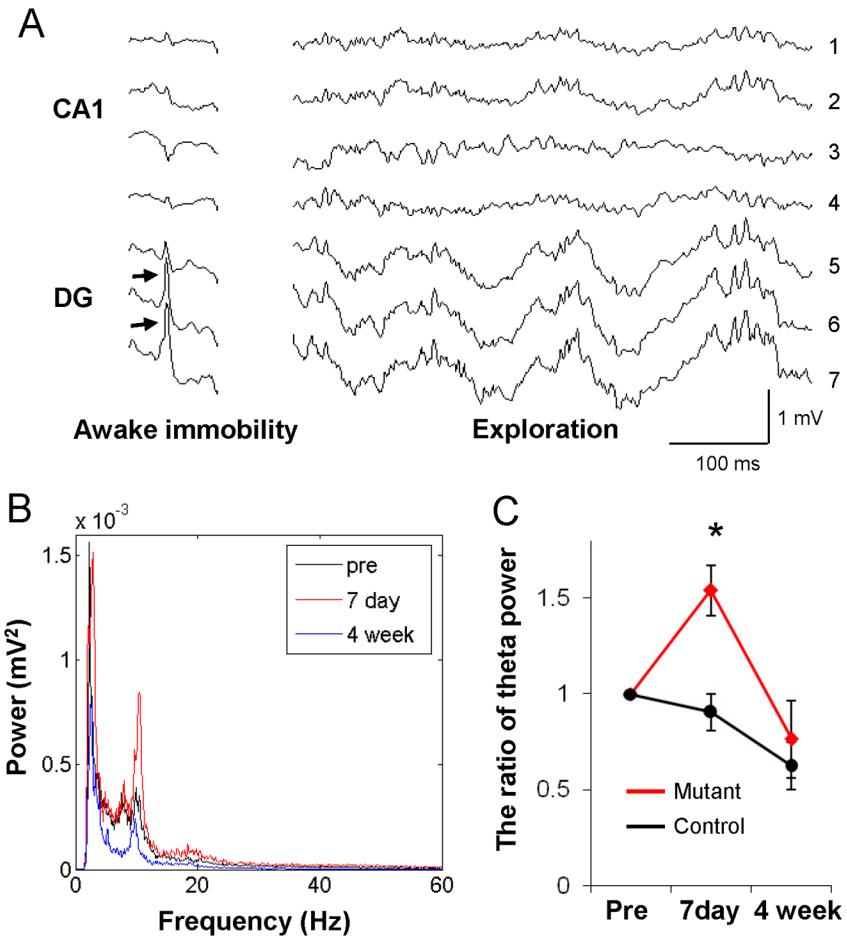

Figure 7. Transient increase in theta oscillatory powers in acute phase

(A) *Field activity in the CA1-dentate axis of hippocampus during awake immobility and exploration (recorded simultaneously from 7 sites at 50–100 μm tip intervals).* Arrows in the granule cell layer or hilar region (electrodes #6 & #7) of dentate gyrus indicate dentate spikes during immobility in control mice. LFP activity containing dentate spikes and large theta-gamma oscillations, typical patterns of which are in electrode #7, were analyzed further. (B) Averaged intensity of 7–12 Hz theta frequency LFP powers during exploration recorded just before DT injection *(pre, black)*, on day 7 *(7 day, red)*, and 4-weeks *(blue)* after treatment from the same electrode (located in the dentate gyrus) in the mutant mouse. (C) The ratio change of theta power (7–12 Hz) intensity across days (pre DT levels as 100%). Mutant mice (n=3, red line) show a transient increase in the theta frequency power at post-DT day 7, whereas the controls do not (n=3, black line), *p<0.05.

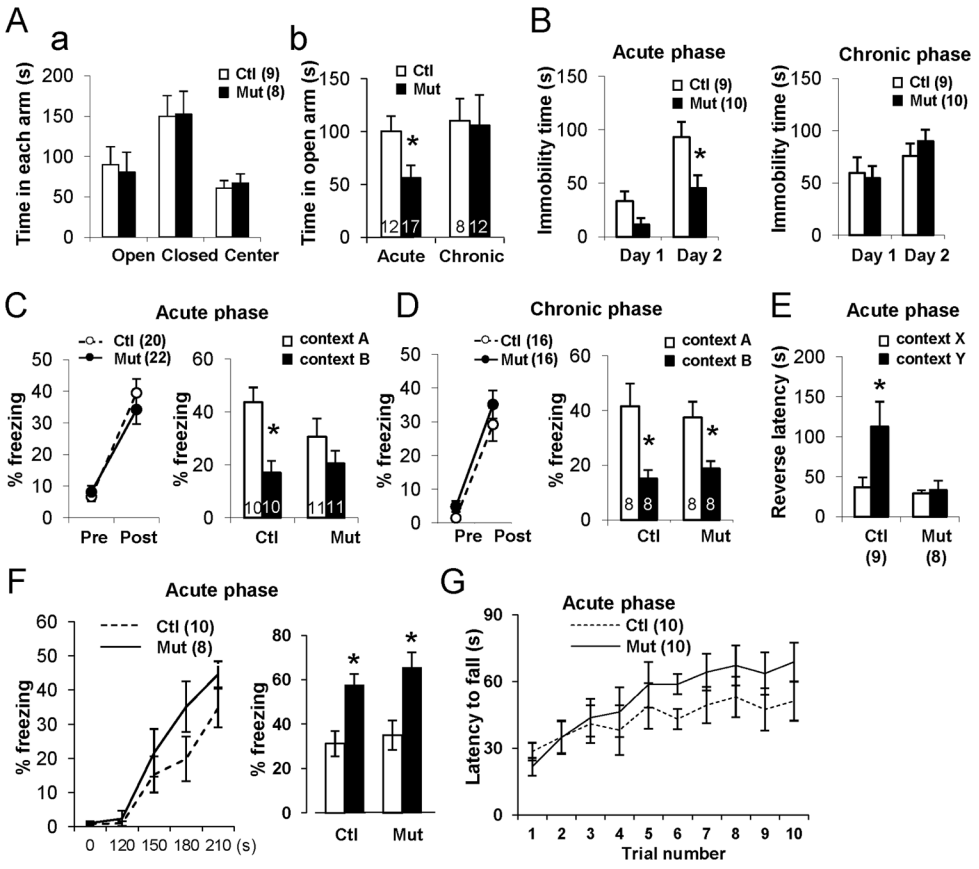

Figure 8. Mossy cell loss followed by increased anxiety and impaired contextual discrimination

(A) Mice with acute-phase mossy cell degeneration show anxiety-like behavior in elevated plus maze. (a) Before DT treatment, no difference by genotype in time spent in each arm of maze. (b) After DT treatment, mutants spend less time in open arm during acute but not chronic phase of DT exposure. *t*-test (**p*<0.05).

(B) Decreased immobility on second day of a 2-day forced swimming test observed in mutants only in acute phase (**p*<0.05).

(C) *Contextual discrimination using one-trial contextual fear conditioning during acute phase. (Left)* Both controls (○) and mutants (●) freeze equally after a single foot shock. *(Right)* 24 hr after learning, mutants but not controls are unable to distinguish context A from context B. Genotype–context interaction F(1, 38)=4.58 (*P*<0.05); Newman–Keuls *post hoc* test (**p*<0.05 for control, *p*=0.29 for mutant).

(D) *One-trial contextual fear conditioning during chronic phase.* 24 hr after foot shock, mutant and control mice both distinguish two contexts. Context effect F(1, 28)=11.1 (p<0.01); Newman–Keuls *post hoc* test (**p*<0.05 for control, **p*<0.05 for mutant).

(E) *Contextual discrimination in one-trial step-through avoidance test during the acute phase.* 24 hr after shock, mutants escape latency from context Y (non-shocked) does not differ from that of context X (shocked), while controls display a longer escape latency from context Y than from context X. Genotype-context interaction, F(1, 30)=4.55 (*p*<0.05). Newman-Keuls *post-hoc* test, X vs Y (**p*<0.05 for control, *p*=0.73 for mutant).

(F) *Cued-fear conditioning.* Delivered during the acute phase, two sets of paired tone (CS) and foot-shocks (US) for conditioning *(Left)* and recall tests 24-hr later *(Right)* before (*white bar*) and during tone presentation (*black bar*) revealed no differences by genotype. Genotype effect, F(1, 34)=0.95. p=0.34, Newman-Keuls *post hoc* test (**p*<0.02 for both genotypes).

(G) As assessed by the accelerating rotarod test, balance and motor coordination in mutants and controls was normal. Animal number is indicated in parentheses or plot bars.